



## Multivariate recurrence plots

M. Carmen Romano<sup>a,\*</sup>, Marco Thiel<sup>a</sup>, Jürgen Kurths<sup>a</sup>, Werner von Bloh<sup>b</sup>

<sup>a</sup> *University of Potsdam, Nonlinear Dynamics, Am Neuen Palais 10, 14469 Potsdam, Germany*

<sup>b</sup> *Potsdam Institute for Climate Impact Research, Telegrafenberg A31, 14473 Potsdam, Germany*

Received 19 May 2004; received in revised form 27 July 2004; accepted 28 July 2004

Communicated by C.R. Doering

### Abstract

We propose a new approach to calculate recurrence plots of multivariate time series, based on joint recurrences in phase space. This new method allows to estimate dynamical invariants of the whole system, like the joint Rényi entropy of second order. We use this entropy measure to quantitatively study in detail the phase synchronization of two bidirectionally coupled chaotic systems and identify different types of transitions to chaotic phase synchronization in dependence on the coupling strength and the frequency mismatch. By means of this analysis we find several new phenomena, such a chaos–period–chaos transition to phase synchronization for rather large coupling strengths.

© 2004 Elsevier B.V. All rights reserved.

### 1. Introduction

Recurrence plots (RPs) is a method of analysis of data that was initially introduced to visualize the behavior of a trajectory of a dynamical system in phase space [5]. In order to go beyond the visual impression, different measures of quantification of RPs were introduced later [27]. This technique has been successfully applied to various fields, such as physiology [9,29], fluid dynamics [26] or geology [8]. Further, this technique was enhanced to analyze the relation-

ship between two different dynamical systems, called cross recurrence plot (CRP) [28]. The main advantage of this technique with respect to other nonlinear data analysis methods, is that it can be applied to nonstationary and rather short time series [5,9,10,20,30].

In this Letter we propose another approach to calculate multivariate recurrence plots, that enables to estimate invariants of the dynamics and information measures. Furthermore, we show that this modified method is a useful tool to identify complex synchronization phenomena and to determine weak coupling strengths between two different systems, like in the case of phase synchronization.

The outline of this Letter is as follows: first, we motivate the multivariate RPs and introduce an estimator

\* Corresponding author.

E-mail address: [romano@agnld.uni-potsdam.de](mailto:romano@agnld.uni-potsdam.de)  
(M.C. Romano).

of the joint Rényi entropy based on joint recurrences in phase space. To illustrate some potentials of our method, we apply it to two non-identical chaotic oscillators that are bidirectionally coupled and undergo a transition to phase synchronization (PS) [11] for a certain range of parameter values. We then show that this new technique is not only able to detect PS, but it also reveals detailed structures in the parameter space of the whole system, like, e.g., different types of transitions to PS.

## 2. Multivariate recurrence plots

In this section we recall the definition of the cross mutual information as a motivation for a new approach to compute multivariate RPs.

Roughly speaking, mutual information quantifies the amount of information we obtain from the measurement of one random variable on another one. Hence, it has become a widely applied measure to quantify linear and nonlinear dependencies within or between time series (auto, respectively, cross mutual information) [14]. Suppose that we have two dynamical systems represented by the orbits  $\vec{x}_i$  and  $\vec{y}_i$ , with  $i = 1, \dots, N$ . We can associate them with probability distributions  $\{p_m\}_{m=1}^M$ ,  $\{q_n\}_{n=1}^N$  and the joint probability distribution  $\{s_{m,n}\}_{m,n=1}^{M,N}$  [2]. Then the generalized mutual information (GMI) of second order [13] is given by

$$I_2(\vec{x}, \vec{y}) = H_2(\vec{x}) + H_2(\vec{y}) - H_2(\vec{x}, \vec{y}), \quad (1)$$

where  $H_2$  denotes the Rényi information of second order [2], which is defined by

$$H_2(\vec{x}) = -\log \sum_{m=1}^M p_m^2. \quad (2)$$

Substituting (2) in Eq. (1) we obtain

$$I_2(\vec{x}, \vec{y}) = -\log \sum_{m=1}^M p_m^2 - \log \sum_{n=1}^N q_n^2 + \log \sum_{m,n=1}^{M,N} s_{m,n}^2. \quad (3)$$

It is also possible to consider this measure in dependence on a time delay, i.e.,

$$I_2(\vec{x}(t), \vec{y}(t + \tau)) = H_2(\vec{x}(t)) + H_2(\vec{y}(t)) - H_2(\vec{x}(t), \vec{y}(t + \tau)), \quad (4)$$

and especially, to regard the auto mutual information (AMI)

$$AI_2(\vec{x}(t), \vec{x}(t + \tau)) = 2H_2(\vec{x}(t)) - H_2(\vec{x}(t), \vec{x}(t + \tau)). \quad (5)$$

Thiel et al. [25] have recently shown, that it is possible to estimate the Rényi information and the auto mutual information by means of RPs. For example, the second order Rényi information can be estimated as follows

$$\hat{H}_2(\vec{x}, \varepsilon) = -\log \left( \frac{1}{N^2} \sum_{i,j=1}^N R_{i,j} \right), \quad (6)$$

where  $R_{i,j}$  is the recurrence matrix defined by

$$R_{i,j} = \Theta(e - \|\vec{x}_i - \vec{x}_j\|), \quad (7)$$

and  $\Theta(\cdot)$  denotes the Heaviside function and  $\varepsilon$  a pre-defined threshold. They have also shown that the joint Rényi information that enters in the formula for the auto mutual information can be estimated by

$$\hat{H}_2(\vec{x}(t), \vec{x}(t + \tau), \varepsilon) = -\log \left( \frac{1}{(N - \tau)^2} \sum_{i,j=1}^{N-\tau} R_{i,j} R_{i+\tau,j+\tau} \right). \quad (8)$$

Analogously, we can now estimate the joint information and substitute it in Eq. (1),

$$\begin{aligned} \hat{H}_2(\vec{x}(t), \vec{y}(t), \varepsilon_x, \varepsilon_y) &= -\log \left( \frac{1}{N^2} \sum_{i,j=1}^N R_{i,j}^x R_{i,j}^y \right) \\ &= -\log \left( \frac{1}{N^2} \sum_{i,j=1}^N \Theta(\varepsilon_x - \|\vec{x}_i - \vec{x}_j\|) \right. \\ &\quad \left. \times \Theta(\varepsilon_y - \|\vec{y}_i - \vec{y}_j\|) \right), \end{aligned} \quad (9)$$

where  $R_{i,j}^x$  and  $R_{i,j}^y$  represent the recurrence matrices of  $\vec{x}_i$ , respectively,  $\vec{y}_i$ . More generally, if we consider the generalized mutual information function in dependence on the time delay (Eq. (4)), we estimate the joint Rényi information  $H_2(\vec{x}(t), \vec{y}(t + \tau))$  by

$$\begin{aligned}
& H_2(\vec{x}(t), \vec{y}(t + \tau), \varepsilon_x, \varepsilon_y) \\
&= -\log\left(\frac{1}{(N - \tau)^2} \sum_{i,j=1}^{N-\tau} \Theta(\varepsilon_x - \|\vec{x}_i - \vec{x}_j\|) \right. \\
&\quad \left. \times \Theta(\varepsilon_y - \|\vec{y}_{i+\tau} - \vec{y}_{j+\tau}\|)\right). \quad (10)
\end{aligned}$$

Note that in order to estimate  $I_2(\vec{x}(t), \vec{y}(t + \tau))$  it is necessary to treat both matrices  $R_{i,j}^x$  and  $R_{i,j}^y$  separately, i.e., we do not *mix* the phase spaces of  $\vec{x}$  and  $\vec{y}$ , in contrast to the definition of the CRP [28]. We rather extend the phase space to  $\mathcal{R}^{d_1+d_2}$ , where  $d_1$  and  $d_2$  are the phase space dimensions of the corresponding systems, and are in general different. Further, we have a different threshold for each system ( $\varepsilon_x$  and  $\varepsilon_y$ ), so that we can apply the criteria to choose them [24,25,29], respecting the natural measure of both systems.<sup>1</sup> Hence it is straightforward to introduce the following *joint recurrence matrix*

$$\begin{aligned}
JR_{i,j}^{x,y} &= \Theta(\varepsilon_x - \|\vec{x}_i - \vec{x}_j\|) \\
&\quad \times \Theta(\varepsilon_y - \|\vec{y}_i - \vec{y}_j\|), \quad i, j = 1, \dots, N, \quad (11)
\end{aligned}$$

i.e.,

$$JR_{i,j}^{x,y} = \begin{cases} 1, & \text{if } \|\vec{x}_i - \vec{x}_j\| < \varepsilon_x \text{ and } \|\vec{y}_i - \vec{y}_j\| < \varepsilon_y, \\ 0, & \text{else.} \end{cases}$$

We propose to consider the matrix  $JR_{i,j}^{x,y}$  as multivariate recurrence plot (MRP). Note that we consider, due to the coupling between the two systems, a single joint phase space of dimension  $d_1 + d_2$ , i.e., all components are orthogonal. We also see, that definition (Eq. (7)) of an RP is a special case of the definition (Eq. (11)) if we have only one system. In our approach a recurrence takes place if one point of the trajectory  $\vec{x}_j$  for  $j = 1, 2, \dots$  returns to the neighborhood of the point  $\vec{x}_i$  in phase space, and simultaneously one point of the trajectory  $\vec{y}_j$  for  $j = 1, 2, \dots$  returns to the neighborhood of the point  $\vec{y}_i$ . That means, we consider the joint probability that both recurrences happen simultaneously. In contrast, in CRPs recurrence is defined when a point of the trajectory  $\vec{x}_i$  is within one  $\varepsilon$ -neighborhood of the point of the trajectory  $\vec{y}_j$ .

<sup>1</sup> Note that it is also possible to choose  $(d_1 + d_2)$  different values  $\varepsilon_i$ , one for each coordinate of the whole phase space, or one threshold for all components.

### 3. Estimation of the joint Rényi entropy of second order

Thiel et al. [25,26] have recently shown that it is possible to estimate some dynamical invariants by means of RPs, like the second order Rényi entropy  $K_2$ ,  $AI_2$  and the generalized dimension of second order  $D_2$ . In this Letter, we extend these estimators to 2-dimensional systems, considering the joint probabilities of recurrences (e.g., we have shown in Section 2 that  $I_2(\vec{x}(t), \vec{y}(t + \tau))$  can be estimated by means of MRPs). Here we focus on the joint  $K_2$ , which is defined as

$$\begin{aligned}
K_2 &= -\lim_{\Delta t \rightarrow 0} \lim_{\varepsilon \rightarrow 0} \lim_{l \rightarrow \infty} \frac{1}{l \Delta t} \\
&\quad \times \log \sum_{i_1, \dots, i_l, j_1, \dots, j_l} p^2(i_1, \dots, i_l, j_1, \dots, j_l), \quad (12)
\end{aligned}$$

where  $p(i_1, i_2, \dots, i_l, j_1, j_2, \dots, j_l)$  is the joint probability that  $\vec{x}(\Delta t)$  is in box  $i_1$ ,  $\vec{x}(2\Delta t)$  is in box  $i_2, \dots, \vec{x}(l\Delta t)$  is in box  $i_l$  and *simultaneously*  $\vec{y}(\Delta t)$  is in box  $j_1$ ,  $\vec{y}(2\Delta t)$  is in box  $j_2, \dots$ , and  $\vec{y}(l\Delta t)$  is in box  $j_l$ . Then we can estimate  $K_2$  in terms of MRPs by

$$\begin{aligned}
& \hat{K}_2(\varepsilon_x, \varepsilon_y, l) \\
&= \frac{1}{l \Delta t} \log \left( \frac{1}{N^2} \sum_{t,s=1}^N \prod_{m=0}^{l-1} JR_{t+m,s+m}^{x,y} \right). \quad (13)
\end{aligned}$$

Note that the term

$$\frac{1}{N^2} \sum_{t,s=1}^N \prod_{m=0}^{l-1} JR_{t+m,s+m}^{x,y}$$

is the probability  $P_{\varepsilon_x, \varepsilon_y}(l)$  to find a diagonal line of at least length  $l$  in the MRP. Hence, representing logarithmically the histogram of diagonals of length  $l$  versus  $l$ , the slope of the distribution is an estimator for the joint Rényi entropy. In the following we show that this measure estimated from MRPs is a powerful tool for the analysis of complex synchronization phenomena.

### 4. Detection of synchronization transition by means of joint recurrences

Phase synchronization (PS) of chaotic systems has been recently extensively studied [4,11,12,15,22] and

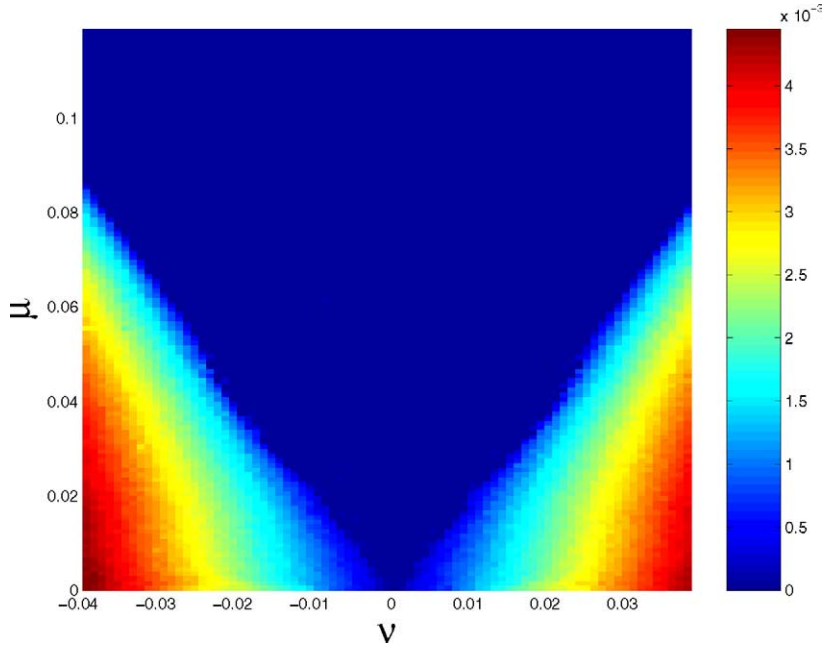


Fig. 1. Difference  $|\Delta\Omega|$  between the mean frequencies of the two Rössler oscillators (Eq. (14)) in dependence on the frequency mismatch and coupling strength.

found applications in many fields [3,17,23]. In this section we estimate the joint  $K_2$  by means of MRPs for the prototypical chaotic case of two mutually coupled Rössler oscillators

$$\begin{aligned}
 \dot{x}_1 &= -(1 + \nu)x_2 - x_3 + \mu(y_1 - x_1), \\
 \dot{x}_2 &= (1 + \nu)x_1 + 0.15x_2, \\
 \dot{x}_3 &= 0.2 + x_3(x_1 - 10), \\
 \dot{y}_1 &= -(1 - \nu)y_2 - y_3 + \mu(x_1 - y_1), \\
 \dot{y}_2 &= (1 - \nu)y_1 + 0.15y_2, \\
 \dot{y}_3 &= 0.2 + y_3(y_1 - 10),
 \end{aligned} \tag{14}$$

where the parameter  $\nu$  governs the detuning of the frequencies and the coupling is diffusive and proportional to the coupling strength  $\mu$ .<sup>2</sup> We analyze the following range of parameters, where the two oscillators undergo transitions to phase synchronization:  $\nu = -0.04, \dots, 0.04$  and  $\mu = 0.0, \dots, 0.12$ . In Fig. 1 the difference of the mean frequencies  $\Delta\Omega = \Omega_1 - \Omega_2$

of the two oscillators shows the well-known Arnold tongue.<sup>3</sup> Now we estimate the joint  $K_2$  based on MRPs in the same parameter range (for a detailed description of the computation, see Appendix A). The results, represented in Fig. 2, also reflect this, but they exhibit more details than Fig. 1:

- First, we see two “borders” in the upper part of Fig. 2 ( $\mu > 0.04$ ): the outer ones correspond to the border of the Arnold tongue, i.e., inside this border the oscillators are in PS, whereas outside they are not. Both borders have very low values of  $\hat{K}_2$ , i.e., the behavior of the system is rather regular there, even periodic in small regions on both borders. This is a remarkable fact, because it means that for relative high coupling strengths the transition to PS is a chaos–period–chaos one, as inside the tongue  $\hat{K}_2 > 0$ , indicating a chaotic regime.
- Inside the Arnold tongue, for coupling strengths  $\mu$  between approximately 0.025 and 0.04, we find a region (which looks like two eyes), where the

<sup>2</sup> The system was integrated using Runge–Kutta of fourth order. The integration step is  $h = 0.01$  and the sampling time  $s = 20$ , so that the time interval between two consecutive points is  $\Delta t = 0.2$ .

<sup>3</sup> The mean frequencies  $\Omega_1$  and  $\Omega_2$  were calculated following [11].

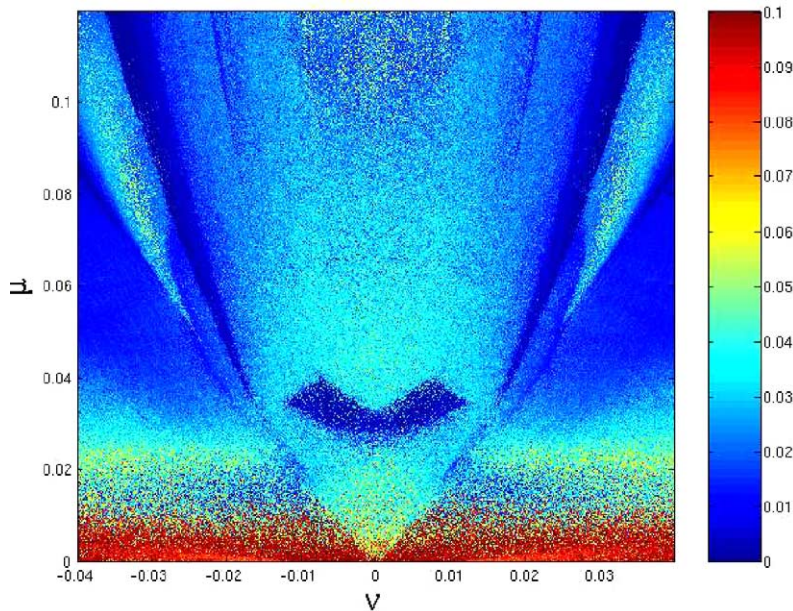


Fig. 2. Joint Rényi entropy  $\hat{K}_2$  of the two Rössler oscillators in dependence on the frequency mismatch and coupling strength.

value of  $\hat{K}_2$  is (almost) 0, i.e., the region is periodic.

- For  $\mu > 0.03$  the region inside the Arnold tongue is more chaotic (larger  $\hat{K}_2$ ) than outside the tongue. This is surprising, as one would expect that if both oscillators are synchronized, the behavior of the whole system becomes more and more regular for increasing coupling.

#### 4.1. Comparison between the sum of the positive Lyapunov exponents and $K_2$

In order to validate these results, we calculate the Lyapunov spectrum of the whole system based on Eq. (14), i.e., it is *not* estimated from the time series. As  $K_2$  is bounded from above by the sum of the positive Lyapunov exponents [2,18], we should obtain qualitatively the same structures plotting  $\sum_{\lambda_i > 0} \lambda_i$  in the considered parameter space as in Fig. 2. Indeed, the structures in Fig. 3 are reproduced in Fig. 2. It is remarkable, that  $K_2$  was estimated from time series with 10 000 data points (see Appendix A for the details of the computation), whereas for the computation of the sum of the positive Lyapunov exponents, Eq. (14) were used. As we are interested in a method for data analysis, where the equations governing the system are

usually not known, the technique to estimate the predictability of the system in parameter space based on MRPs seems to yield confident results.

It is important to note that we observe one qualitative difference between Fig. 2 and Fig. 3: for  $\mu \in [0, 0.006]$  one cannot distinguish the tip of the Arnold tongue only by considering the sum of the positive Lyapunov exponents (see Fig. 5), whereas taking into account  $\hat{K}_2$  one does (Fig. 4). This is due to the fact, that the relationship  $K_2 = \sum_i \lambda_i^+$  is only true for hyperbolic systems but the 6-dimensional system (Eq. (14)) is not a hyperbolic one. For nonhyperbolic systems,  $K_2 \leq \sum_i \lambda_i^+$  holds [18]. Hence, we have shown that  $K_2$  can provide important complementary information to the sum of the positive Lyapunov exponents.

#### 4.2. Different types of transitions to PS

By means of the joint recurrences, we have detected different transitions to PS for the two coupled Rössler systems in dependence on the coupling strength (Fig. 2): for lower  $\mu$ , a chaos–chaos transition occurs and the whole system is less chaotic in the phase synchronized state than in the non-phase synchronized one. In contrast, for higher  $\mu$  a chaos–

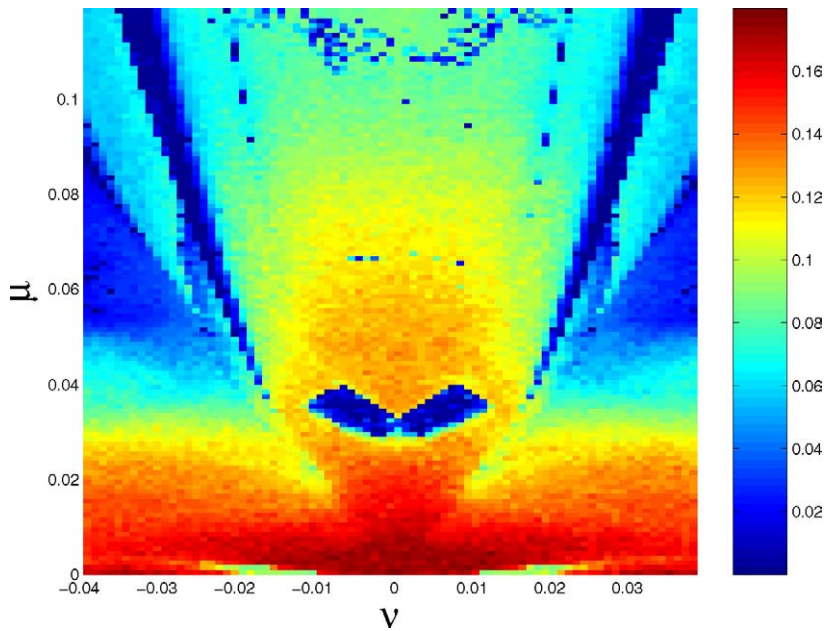


Fig. 3. Sum of the positive Lyapunov exponents of the two Rössler oscillators in dependence on the frequency mismatch and coupling strength.

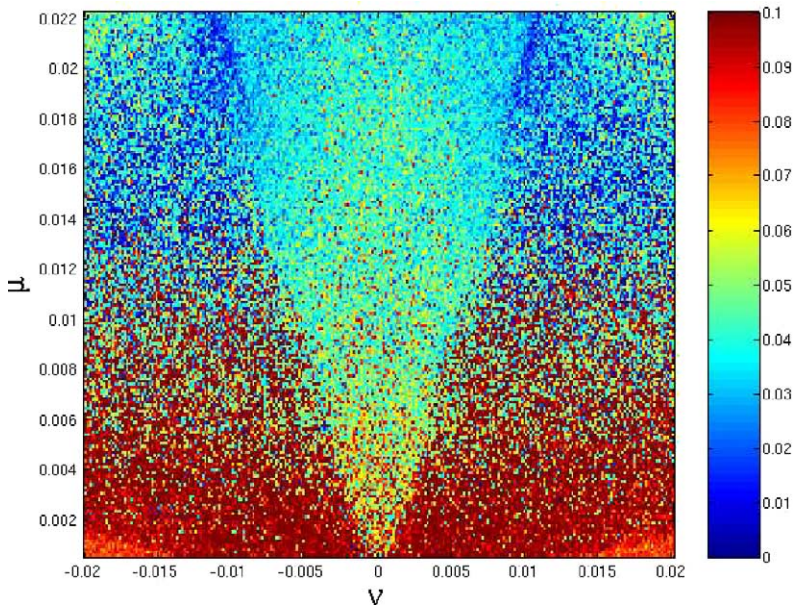


Fig. 4. Zoom of the joint Rényi entropy  $\hat{K}_2$  of the two Rössler oscillators (Eq. (14)) in dependence on the frequency mismatch for low values of the coupling strength.

period–chaos transition is observed and the system is more chaotic in the phase synchronized regime than in the non-phase synchronized one.

In the literature, it is often claimed that all transitions between different types of synchronization can be related to the changes in the Lyapunov spec-

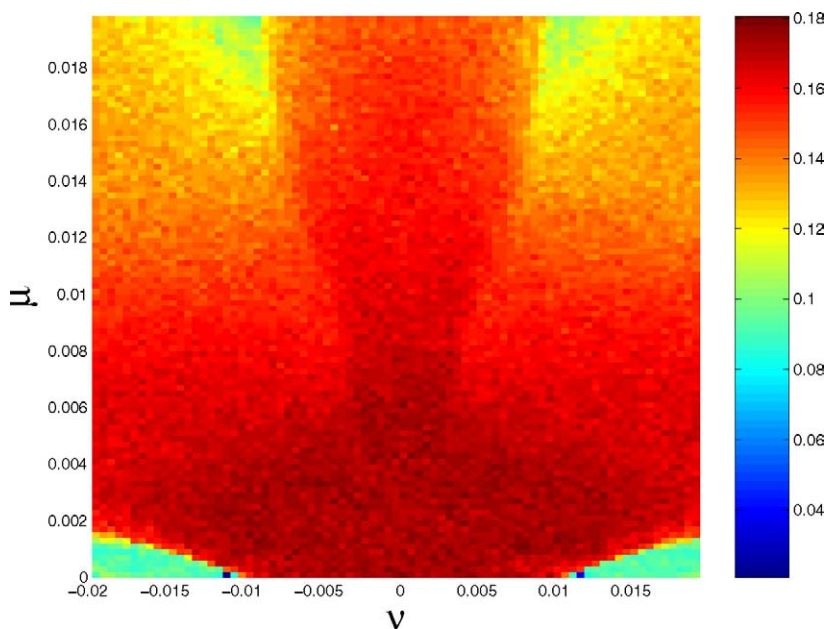


Fig. 5. Zoom of the sum of the positive Lyapunov exponents of the two Rössler oscillators in dependence on the frequency mismatch for low values of the coupling strength.

trum [16]: for rather low values of the coupling strength, one has the following configuration:  $\{\lambda_1 > 0, \lambda_2 > 0, \lambda_3 \sim 0, \lambda_4 \sim 0, \lambda_5 < 0, \lambda_6 < 0\}$ . Increasing the coupling strength,  $\lambda_4$  becomes negative, indicating the transition to PS. If one continues increasing  $\mu$ , then  $\lambda_2 \sim 0$  and  $\lambda_3 < 0$ , indicating the transition to generalized synchronization (GS) [19], where not only the phases, but also the amplitudes become correlated.

In order to relate this theory with our results obtained by means of  $K_2$  in the case of Eq. (14), we code the different configurations of the Lyapunov spectrum in colors (Fig. 6). The conclusions we can draw from Fig. 6 are:

- For  $0.031 < \mu < 0.055$  PS is not reflected any more by the change of  $\lambda_4$  to negative values. In this region  $\lambda_4$  is negative also outside the Arnold tongue. This means, that for these values of  $\mu$ , the phases of both subsystems are not independent any more. However, this dependence is still weak, and  $\phi_1 - \phi_2$  is not constant, so that both subsystems are not in PS for large frequency mismatch.
- For  $0.055 < \mu < 0.1$  we observe GS for large values of the frequency mismatch. That means, outside and on the edge of the Arnold tongue, we

find GS, and decreasing the frequency mismatch (going in the horizontal direction), the correlation between the amplitudes also decreases, as we only have PS and not GS. This is in accordance with the upper part of Figs. 2 and 3, where inside the tongue, the whole system is more chaotic than outside.

- We see two “borders” of the Arnold tongue (red points): the inner one is periodic and the outer one is exactly periodic only for  $\mu$  larger than about 0.8. This also in accordance with the results of Fig. 2.

## 5. Conclusions

In this Letter, we have proposed a modified method to compute multivariate RPs (MRPs). The altered method of MRPs is based on joint recurrences in phase space and allows to estimate easily the joint Rényi entropy of second order  $K_2$ .

We have applied  $K_2$  estimated by means of MRPs to the paradigmatic system of two bidirectionally coupled Rössler systems. There we have detected three different types of transitions to phase synchronization.

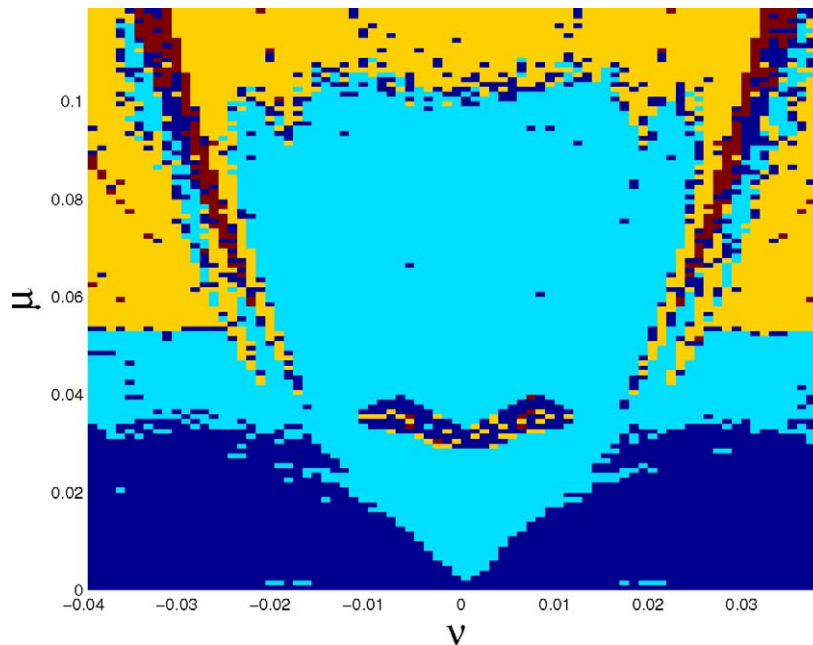


Fig. 6. Different configurations of the Lyapunov spectrum are coded with different colors: dark blue:  $\{\lambda_1 > 0, \lambda_2 > 0, \lambda_3 \sim 0, \lambda_4 \sim 0\}$ , light blue:  $\{\lambda_1 > 0, \lambda_2 > 0, \lambda_3 \sim 0, \lambda_4 < 0\}$ , yellow:  $\{\lambda_1 > 0, \lambda_2 \sim 0, \lambda_3 < 0, \lambda_4 < 0\}$  and red:  $\{\lambda_1 \sim 0, \lambda_2 < 0, \lambda_3 < 0, \lambda_4 < 0\}$ . (For interpretation of the references to colour in this figure legend, the reader is referred to the web version of this Letter.)

To validate this result, we have compared the estimated  $K_2$  with the sum of the positive Lyapunov exponents. Qualitatively we have obtained the same structures in the parameter space. However, for rather small coupling strengths,  $K_2$  can detect the transition to PS, whereas the sum of the positive Lyapunov exponents cannot, due to the nonhyperbolicity of the considered system. Hence, the estimate of  $K_2$  by means of MRPs is a powerful tool for the analysis of the mean predictability of dynamical systems, especially when no model equations of the underlying system is available.

On the other hand, we have calculated the Lyapunov spectrum  $\{\lambda_i\}$  for the whole range of parameters considered. Coding the different configurations of  $\{\lambda_i\}$  with different colors, we have seen that for intermediate coupling strengths, outside the Arnold tongue one zero Lyapunov exponent has passed to negative values. That means, in this range of parameters the phases become already weakly correlated, although they are not locked. These findings challenge for an extension of the theory of complex synchronization. Beyond this, applying the former method of CRPs to the same example, we could not distinguish between PS and

non-PS. However, we want to emphasize that CRPs have other advantages with respect to MRPs. For example, CRPs have been applied very successfully to the readjustment of geological time series with different time scales [8]. Hence, depending on the problem, one has to select the more appropriate one.

We plan to develop the analysis of the influence of noise to the presented algorithm. First steps in this direction are presented in [24]. Furthermore, we plan to apply the proposed method to measured daily temperature data on one hand, and to EEG and eye-movement time series on the other hand, to compare the outcomes with saccade generation models [6].

### Acknowledgements

We want to thank the Helmholtz School and the “Promotionskolleg Computational Neuroscience of Behavioral and Cognitive Dynamics” supported by the Ministerium für Wissenschaft, Forschung und Kultur Brandenburg and the “DFG-Schwerpunkt 1114” for supporting this work.



## Appendix A. Automatization of the algorithm

To compute the joint Rényi entropy  $K_2$  (Eq. (12)) in the whole range of parameters  $\nu \in [-0.04, 0.04]$  and  $\mu \in [0.0, 0.12]$ , the algorithm based on MRPs (Eq. (11)) had to be automated. First, the distribution of diagonal lines for different thresholds  $\varepsilon$  has to be computed, as the entropy is only well defined when a scaling region with  $\varepsilon$  is found. In the case of MRPs we have in general two thresholds  $\varepsilon_x$  and  $\varepsilon_y$ . As there exists a unique relationship between the threshold and the recurrence rate  $RR$  [25,26],<sup>4</sup> we use different values of  $RR$ , because they are normed. The crucial point in the automatization is the estimation of the scaling region of  $\ln P_{RR}(l)$  vs.  $l$  and the plateau in  $K_2(RR)$  vs.  $RR$ . In both cases we applied a cluster dissection algorithm [21]. The algorithm divides the set of points into distinct clusters. In each cluster a linear regression is performed. The algorithm minimizes the sum of all square residuals in order to determine the scaling region and the plateau. To find both regions automatically, we used the following parameters:

- We considered only diagonal lines up to length  $l_{\max} = 400$ . Longer lines were excluded because of finite size effects.
- We considered only values of  $P_{RR}(l)$  with  $P_{RR}(l) > 500$  for the same reason as in the last item.
- We used 40 different values for  $\varepsilon_x$  and  $\varepsilon_y$ , corresponding to 40 equally spaced recurrence rates  $RR$  between 1% and 95%, to have a good defined plateau in  $K_2(RR)$  vs.  $RR$ .
- We used 10000 data points of each simulated trajectory. The more data points one uses, the more pronounced the scaling regions. Note that the computation time increases approximately with  $N^2$ .
- We had to specify for the applied cluster dissection algorithm the number of clusters in each run:

for the detection of the scaling region in  $\ln P_{RR}(l)$  vs.  $l$ , we chose 2 different clusters and used the slope of the largest cluster. For the detection of the plateau in  $K_2(RR)$  vs.  $RR$ , we chose 3 clusters and used the value of the cluster with the minimum absolute slope.

These choices have proven to be the most appropriate ones for the estimation of the scaling regions. All these parameters are defaults of a computer program. Furthermore, this automatization of the algorithm has been already successfully applied to the computation of stability of trajectories of extrasolar planetary systems [1].

## References

- [1] N. Asghari, et al., Stability of terrestrial planets in the habitable zone of GI 777 A, HD 72659, GI 614, 47 Uma and HD 4208, *Astron. Astrophys.*, in press.
- [2] C. Beck, F. Schlögl, *Thermodynamics of Chaotic Systems: An Introduction*, in: Cambridge Nonlinear Science Series, 1992.
- [3] B. Blasius, A. Huppert, L. Stone, *Nature* 399 (1999) 354.
- [4] S. Boccaletti, J. Kurths, G. Osipov, D.L. Valladares, C.S. Zhou, *Phys. Rep.* 366 (2002) 1.
- [5] J.-P. Eckmann, S.O. Kamphorst, D. Ruelle, *Europhys. Lett.* 4 (1987) 973.
- [6] R. Engbert, A. Longtin, R. Kliegl, *Vision Res.* 42 (2002) 621.
- [7] P. Grassberger, I. Procaccia, *Physica D* 9 (1983) 189.
- [8] N. Marwan, M. Thiel, N.R. Nowaczyk, *Nonl. Processes Geophys.* 9 (3/4) (2002) 325.
- [9] N. Marwan, N. Wessel, J. Kurths, *Phys. Rev. E* 66 (2) (2002) 026702.
- [10] N. Marwan, J. Kurths, *Phys. Lett. A* 302 (5–6) (2002) 299.
- [11] A. Pikovsky, M. Rosenblum, J. Kurths, *Synchronization*, Cambridge Univ. Press, Cambridge, 2001.
- [12] A. Pikovsky, M. Rosenblum, G. Osipov, J. Kurths, *Physica D* 104 (1997) 219.
- [13] B. Pompe, *J. Stat. Phys.* 73 (1993) 587.
- [14] B. Pompe, P. Blihd, D. Hoyer, M. Eiselt, *IEEE Eng. Med. Biol. Mag.* 17 (1998) 32.
- [15] M. Rosenblum, A. Pikovsky, J. Kurths, *Phys. Rev. Lett.* 76 (1996) 1804.
- [16] M. Rosenblum, A. Pikovsky, J. Kurths, *Phys. Rev. Lett.* 78 (1997) 4193.
- [17] M. Rosenblum, L. Cimponeriu, A. Bezerianos, A. Patzak, R. Mrowka, *Phys. Rev. E* 65 (2002) 041909.
- [18] D. Ruelle, *Bol. Soc. Brasil. Mat.* 9 (1978) 3.
- [19] N.F. Rulkov, M.M. Sushchik, L.S. Tsimring, H.D.I. Abarbanel, *Phys. Rev. E* 51 (2) (1995) 980.
- [20] K. Shockley, M. Butwill, J.P. Zbilut, C.L. Webber Jr., *Phys. Lett. A* 305 (2002) 59.

<sup>4</sup> The recurrence rate  $RR$  is defined as the percentage of black points in the RP, i.e.,

$$RR = \frac{1}{N^2} \sum_{i,j=1}^N \Theta(\varepsilon - \|\vec{x}_i - \vec{x}_j\|).$$

Note, that the definition of  $RR$  coincides with the one of the correlation sum [7].

- [21] H. Späth, *Cluster Dissection and Analysis*, Ellis Horwood, Chichester, 1992.
- [22] O.V. Sosnovtseva, A.C. Balanov, T.E. Vadisova, V.V. Asthakov, E. Mosekilde, *Phys. Rev. E* 60 (1999) 6560.
- [23] P. Tass, M. Rosenblum, J. Weule, J. Kurths, A. Pikovsky, J. Volkmann, A. Schnitzler, H.-J. Freund, *Phys. Rev. Lett.* 81 (15) (1998) 3291.
- [24] M. Thiel, M.C. Romano, J. Kurths, R. Meucci, E. Allaria, T. Arecchi, *Physica D* 171 (3) (2002) 138.
- [25] M. Thiel, M.C. Romano, J. Kurths, *Appl. Nonlin. Dyn.* 11 (3) (2003) 20.
- [26] M. Thiel, M.C. Romano, P. Read, J. Kurths, *Chaos* 14 (2) (2004) 234.
- [27] C.L. Webber Jr., J.P. Zbilut, *J. Appl. Physiol.* 76 (1994) 965.
- [28] J.P. Zbilut, A. Giuliani, C.L. Webber Jr., *Phys. Lett. A* 246 (1998) 122.
- [29] J.P. Zbilut, N. Thomasson, C.L. Webber, *Med. Eng. Phys.* (2002).
- [30] J.P. Zbilut, A. Giuliani, C.L. Webber Jr., *Phys. Lett. A* 246 (1998) 122.